

AAPM Task Group 128: Quality assurance tests for prostate brachytherapy ultrasound systems

Douglas Pfeiffer^{a)}

Imaging Department, Boulder Community Foothills Hospital, Boulder, Colorado 80301

Steven Sutlief

Radiation Therapy, VA Medical Center, VA Puget Sound Health Care System, Seattle, Washington 98108

Wenzheng Feng

Cardiology and Interventional Radiology, William Beaumont Hospital, Royal Oak, Michigan 48073

Heather M. Pierce

CIRS, Inc., Norfolk, Virginia 23513

Jim Kofler

Radiology, Mayo Clinic, Rochester, Minnesota 55905

(Received 26 December 2007; revised 27 August 2008; accepted for publication 6 October 2008; published 12 November 2008)

While ultrasound guided prostate brachytherapy has gained wide acceptance as a primary treatment tool for prostate cancer, quality assurance of the ultrasound guidance system has received very little attention. Task Group 128 of the American Association of Physicists in Medicine was created to address quality assurance requirements specific to transrectal ultrasound used for guidance of prostate brachytherapy. Accurate imaging guidance and dosimetry calculation depend upon the quality and accuracy of the ultrasound image. Therefore, a robust quality assurance program for the ultrasound system is essential. A brief review of prostate brachytherapy and ultrasound physics is provided, followed by a recommendation for elements to be included in a comprehensive test phantom. Specific test recommendations are presented, covering grayscale visibility, depth of penetration, axial and lateral resolution, distance measurement, area measurement, volume measurement, needle template/electronic grid alignment, and geometric consistency with the treatment planning computer. © 2008 American Association of Physicists in Medicine.

[DOI: [10.1118/1.3006337](https://doi.org/10.1118/1.3006337)]

Key words: prostate, brachytherapy, implant, ultrasound, quality assurance, quality control, phantoms

TABLE OF CONTENTS

I. INTRODUCTION.	5472	II.F.1. Recommended frequency: Annual.	5480
I.A. Prostate brachytherapy.	5472	II.G. Test 7: Needle template/electronic grid alignment.	5481
I.B. Ultrasound systems.	5472	II.G.1. Recommended frequency: The first time a template is used and annually thereafter for preplanned implants, a vendor's disposable templates should be checked periodically for consistency, optional for intraoperative planning.	5481
II. QUALITY CONTROL TESTS.	5475	II.H. Test 8: Treatment planning computer.	5481
II.A. Test 1: Grayscale visibility.	5475	II.H.1. Recommended frequency: Acceptance testing of ultrasound system and/or treatment planning computer.	5481
II.A.1. Recommended frequency: Annual.	5475	III. ARTIFACTS.	5482
II.B. Test 2. Depth of penetration.	5476	IV. QUALITY CONTROL DOCUMENTATION.	5482
II.B.1. Recommended frequency: Annual or following transport to another facility.	5476	V. ADDITIONAL TESTS.	5482
II.C. Test 3. Axial and lateral resolution.	5477	VI. CONCLUSION.	5482
II.C.1. Recommended frequency: Annual or following transport to another facility.	5477	APPENDIX A: DISTANCE CALCULATION.	
II.D. Test 4. Axial and lateral distance measurement accuracy.	5477	1. Axial (vertical) distance measurement.	5482
II.D.1. Recommended frequency: Annual.	5477	2. Lateral (horizontal) distance measurement.	5483
II.D.2. Axial distance accuracy (Fig. 9).	5477	APPENDIX B: POSSIBLE SOURCES OF ERROR.	
II.D.3. Lateral distance accuracy (Fig. 10).	5477	1. Operator-related errors and uncertainties.	5483
II.E. Test 5. Area measurement accuracy.	5480		
II.E.1. Recommended frequency: Annual.	5480		
II.F. Test 6. Volume measurement accuracy.	5480		

2. Phantom-related errors.	5484
3. Scanner-related errors.	5484
APPENDIX C: BOUNDARY DEFINITION.	
1. Boundary definition.	5484
APPENDIX D: REVERBERATION ARTIFACTS.	
1. Reverberation artifacts.	5485
APPENDIX E: SAMPLE QC FORM.	

I. INTRODUCTION

Ultrasound guided prostate brachytherapy has grown in importance as a valuable tool in the treatment of prostate cancer. Often overlooked in a brachytherapy program is the ultrasound system itself, frequently receiving no more attention than, perhaps, a superficial preventive maintenance by a service or biomedical engineer. A comprehensive primer on the brachytherapy procedure is beyond the scope of this work, as is a full, detailed description of a complete quality assurance program for an ultrasound system. The purpose of this document is to provide a set of instructions for quality control testing of an ultrasound system with a specific focus on those tests applicable to image guidance during a prostate implant procedure.

While a brief introduction is provided below, readers unfamiliar with the prostate brachytherapy procedure are referred to the report of the American Association of Physicists in Medicine (AAPM) Task Group No. 64.¹ Further, those readers unfamiliar with ultrasound system quality control testing are referred to the report of AAPM Ultrasound Task Group No. 1.²

A number of different probe stabilizer and stepper systems are commercially available for prostate brachytherapy use. As the focus of this document is ultrasound quality control, quality assurance for these systems will not be discussed. Appropriate quality control tests for stabilization, stepping accuracy, and angulation accuracy should be established by each facility.

It should be noted that ultrasound imaging is highly dependent upon the operator, and substantial changes in target shape, contrast, and resolution can occur with relatively subtle changes in probe position or system setup. It is, therefore, of great importance to ensure consistency from measurement to measurement, and record all relevant parameters to allow them to be reproduced at the next measurement session. Additionally, sources of error must be limited to the degree possible. Appendix B lists some common sources of error.

Throughout this document, the word “axial” is used not as an imaging plane, but in reference to a radial direction from the ultrasound transducer. This is in keeping with the common parlance in ultrasound literature.

I.A. Prostate brachytherapy

While the concept of brachytherapy, the insertion of radioactive sources into a cancerous lesion, has been around since the beginning of the 20th century,³ serious efforts at prostate brachytherapy did not surface until the 1960s.⁴ In the 1980s, use of transperineal needles and transrectal ultra-

sound guidance brought attention to prostate brachytherapy as a viable treatment alternative for prostate cancer.⁵

As opposed to external beam radiation, brachytherapy is performed in a single treatment (or a small number of fractions, in the case of high dose rate brachytherapy). Furthermore, brachytherapy has the ability to achieve a high level of conformity to the prostate, can reduce complications created by radiation to sensitive tissues such as the rectum, and can produce clinical outcomes comparable to external beam radiation and radical prostatectomy. Ultrasound facilitates real time confirmation of needle placement and has great potential in reducing issues with suboptimal seed location. This has the potential to reduce complications in radiosensitive rectum and bladder tissue. Ultrasound-guided prostate seed implant therapy is now well established as an important treatment option for prostate cancer.⁶⁻⁹

Dosimetric planning for prostate brachytherapy falls into two categories: preplans and intraoperative real time planning. With preplans, the plan is based on a preoperative CT or ultrasound image and the seed locations are specified according to grid coordinates. Once in the operating room (OR), seeds, either loose or joined together in strands, are placed within the prostate under ultrasound guidance according to the coordinates specified in the preplan.

When an intraoperative real time planning system is used, a prostate volume study is performed using the transrectal ultrasound. The contours of the prostate in each of the volume study images are transferred to the treatment planning computer and the plan is developed. The seeds are implanted under ultrasound guidance and the plan is modified as needed during the procedure to spare rectal dose or meet other dosimetric goals.

Whether a preoperative plan is used or the dosimetric planning is done real time in the OR, ultrasound guidance is vital for a successful implant. Optimal image quality is central to this. With both preplan and real time planning, it must be possible to insert the needle and seeds within the prostate at the appropriate grid locations, meaning that the electronic grid of the scanner must correspond to the physical grid in the OR. Visualization of the prostate and other critical structures is needed for setup of preplanned implants or for dosimetric calculations of real time planning. Ability to identify the locations of inserted seeds, sometimes assisted by additional imaging techniques such as fluoroscopy, is necessary for both the modification of a preplan in the OR and for real time planning.

I.B. Ultrasound systems

Diagnostic ultrasound (as employed in prostate brachytherapy) is simply the compression and rarefaction of a medium at a frequency in the 3–10 MHz range. The velocity of sound (c) in soft tissue is approximately 1540 m/s. Table I gives the sound speed of some clinically relevant materials. The acoustic impedance (Z) of a material is defined as

TABLE I. Sound speed of selected materials (Ref. 10).

Material	Velocity (m/s)
Air	330
Water	1497
Metal	3000–6000
Fat	1440
Blood	1570
Soft tissue	1540

$$Z = c \times \rho, \quad (1)$$

where ρ is the density of the material. When an ultrasound pulse is transmitted into a material, it is reflected off the interface between two areas of differing impedance. The magnitude of the reflection depends upon the magnitude of the impedance mismatch according, under simplifying assumptions, to

$$\alpha_r = \frac{[Z_2 - Z_1]^2}{[Z_2 + Z_1]^2}, \quad (2)$$

where α_r is the sound power reflection coefficient of a plane wave at normal incidence to a planar interface between two media, and Z_1 and Z_2 are the acoustic impedances of the two materials, respectively.¹¹

The pressure amplitude $P(Z, f)$ of an ultrasound beam is attenuated according to

$$P(Z, f) = P_0 F(f) e^{-\alpha(f)Z}, \quad (3)$$

where f is the ultrasound frequency and $\alpha(f)$ is here the attenuation coefficient. Typical clinical values of Z and f yield $\alpha(f) \approx 0.5 \text{ dB cm}^{-1} \text{ MHz}^{-1}$.¹² Therefore, higher frequency beams are more highly attenuated than lower frequency beams, decreasing the effective depth of penetration (visibility of structures at depth).

As the wavelength of the ultrasound is given by

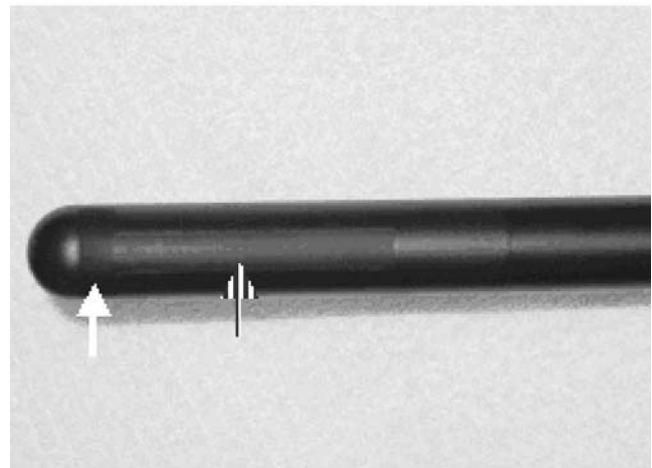
$$\lambda = \frac{c}{f}, \quad (4)$$

it can be seen that ultrasound imaging seeks to optimize a trade off between axial resolution and depth of penetration.

The ultrasound transducer acts as both the transmitter and receiver of the ultrasound pulses. It is an array of small transducer elements that may be addressed individually or in groups. This addressability enables the system to steer and focus the beam. The detailed physics of ultrasound production are beyond the scope of this work. Suffice it to give a simplified description of the process. The transducer transmits ultrasound pulses that are then reflected and scattered within the tissue. The transducer listens for reflected pulses and the two-dimensional image is built up by equating the depth of the reflection r to the time τ it took to receive the reflected pulse according to the range equation



(a)



(b)

FIG. 1. Prostate brachytherapy transrectal ultrasound probe. In (a), note dual connectors required for the orthogonal axial and longitudinal arrays. In (b), the white arrow indicates the axial array and the striped arrow indicates the longitudinal array.

$$r = \frac{c\tau}{2}. \quad (5)$$

Further information regarding beam and image formation is given in other works.¹³

It is important to note that transducers used for guidance during prostate brachytherapy procedures generally incorporate two orthogonal arrays, one sagittal array for base-apex imaging and a transverse array for imaging of the prostate in the orthogonal plane (Fig. 1). Newer transducers may incorporate Doppler capability and a two-dimensional array for simultaneous imaging of sagittal and transverse planes.

Appendix C provides a discussion of how the physics of ultrasound imaging and various image quality factors come together in the clinical task of defining the prostate boundaries.

A quality assurance program is comprised of all of the practices instituted by a facility to ensure that procedures are appropriate, performed according to applicable standards, and are beneficial to improving patient outcomes. One com-



FIG. 2. Test setup. The transrectal ultrasound probe is shown passing under the needle template. Both are fixed to the stepper, which is connected to a stabilizing arm locked to the treatment table. The CIRS Brachytherapy Phantom is used in this example.

ponent of a quality assurance program is quality control testing. Such testing is a series of distinct evaluations to ensure satisfactory performance of a piece of equipment. Quality control testing consists of acceptance testing, which ensures that new equipment or units that have undergone major service perform as expected and are without defects. The acceptance testing also provides a set of baseline performance measures for the equipment to which future measurements are compared. Regular, periodic testing monitors equipment performance to detect changes before they become clinically apparent. Finally, verification of correction is performed following service to ensure that corrective measures have been successfully completed.

Quality control tests of ultrasound imagers typically measure many aspects of image quality and scanner performance.² Additional aspects important to prostate brachytherapy guidance include precise area and volume measurement and needle grid alignment. A brief description of tests that are general to all ultrasound systems is given below, and readers needing more detail are encouraged to see Goodsitt *et al.*² for a complete description. Those tests that are specific to prostate brachytherapy guidance systems are given a complete explanation in this document.

Figure 2 provides a demonstration of the scan setup using a particular phantom and probe support assembly. Figure 3 provides schematics of one commercially available phantom. This phantom is manufactured of Zerdine®, a tissue mimicking material having a sound speed of 1540 m/s. In these images, the test objects discussed below are indicated along with relevant dimensions. These include nylon monofilaments and spherical and nonspherical calibrated volume targets. The trough at the anterior surface of the phantom receives the ultrasound probe and is lined with a tissue mimicking scan surface.

A more comprehensive phantom has been recommended by Task Group 128. The elements of the phantom, listed

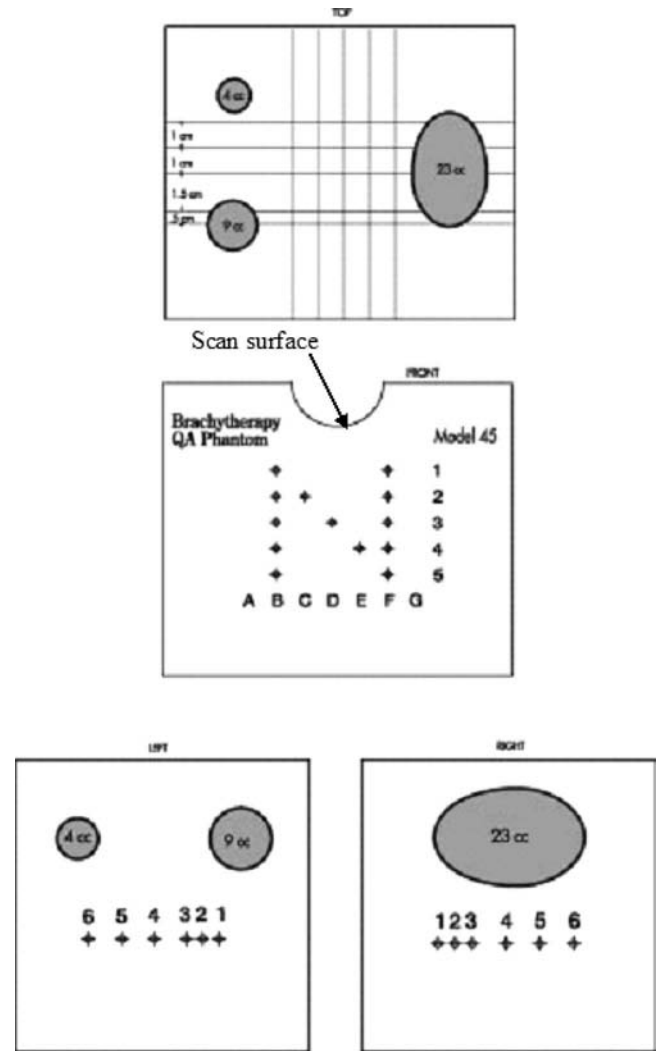


FIG. 3. Phantom schematic. This is the CIRS Model 45 phantom, and is used here for illustrative purposes only; no endorsement is implied.

below, would allow for completion of all of the tests recommended in this document. These elements are:

1. A moderately high contrast volume object, approximately 20–30 cc, preferably egg shaped, for area and volume measurements.
2. A series of midcontrast detail objects for depth of penetration evaluation (diam 6, 4, and 2 mm) going to at least 8 cm.
3. An array of high contrast targets for verification of the electronic grid (2D, approximately 6 cm × 6 cm).
4. An array of high contrast targets in all three orthogonal directions for spatial accuracy verification (possibly shared with the targets in 3).
5. An array of small reflectors for spatial resolution evaluation in two orthogonal directions, near the surface and at depth. These might also be the same as used for 3. and/or 4.
6. Some way of testing the alignment of the physical needle template with the electronic grid.

TABLE II. Quality control tests: frequencies and action levels.

Test	Minimum frequency	Action level
Grayscale visibility	Annual	Change >2 steps or 10% from baseline
Depth of penetration	Annual	Change >1 cm from baseline
Axial and lateral resolution	Annual	Change >1 mm from baseline
Axial distance measurement accuracy	Annual	Error >2 mm or 2%
Lateral distance measurement accuracy	Annual	Error >3 mm or 3%
Area measurement accuracy	Annual	Error >5%
Volume measurement accuracy	Annual	Error >5%
Needle template alignment	Annual	Error >3 mm
Treatment planning computer volume accuracy	Acceptance testing	Error >5%

7. Ability to perform tests in standard clinical configuration (phantom above TRUS probe).
8. An optional line of seed-like objects, in a single longitudinal plane, rotated with respect for each other, to document the dependence of seed visibility on in-plane seed rotation.

As of the date of this publication, no manufacturer has yet produced a phantom with these recommended elements. Several are in the design process, but no production date has been given.

II. QUALITY CONTROL TESTS

For all of the following tests, it is recommended that images be recorded documenting the measurements made. Such a visual record, in either hard copy or digital format, can aid in duplicating the scan setup during future testing. Further, the images can serve as references in case a question regarding image quality arises between the test intervals.

Ideally, tests will be performed by the same individual to eliminate interobserver variability. If several individuals will be responsible for testing, training should take place to improve consistency between observers. In either case, both intra and interobserver variability should be quantified at the outset of the QC program.

Coupling gel must be used to ensure artifact-free contact between the ultrasound probe and the scan surface.

Due to the variety of ultrasound systems available, having substantially different user interfaces, no instructions are provided regarding how to perform specific functions on the ultrasound unit, such as freezing the image or making spatial measurements. It is assumed that the reader has sufficient familiarity with the system to perform these functions.

Suggested test frequencies and action limits are provided in each test description and are summarized in Table II. It should be noted that, while the recommended action limits have been found to be achievable on clinical systems evaluated by the authors, it is possible that a particular unit may be found that cannot meet the recommendation for a specific

test. In this case, the best performance for that unit and that test should be recorded, and the dosimetric consequences of these limitations carefully reviewed by the physicist and discussed with the radiation oncologist, so as to arrive at a decision on the clinical significance of such limitations and whether the unit needs to be replaced.

The suggested frequencies below assume that the system is used at a single facility. If an ultrasound system is frequently transported to different facilities, the testing frequency should be increased. Transporting a system causes stresses and shocks not typically endured that could negatively impact the imaging capabilities of the system. Basic image quality checks as mentioned below should be performed following each move.

II.A. Test 1: Grayscale visibility

II.A.1. Recommended frequency: Annual

While hardcopy images may be used for documentation purposes, intraoperative use of ultrasound during prostate brachytherapy procedures depends primarily upon the live image on the ultrasound system. It is, therefore, imperative that the ultrasound monitor is initially set up properly and remain stable across time. Details of monitor setup and a more in depth discussion of monitor QC are provided elsewhere;² a brief description is provided here. This simplified version relies on the grayscale strip provided along the edge of most ultrasound images.

1. Locate the grayscale strip in the image. These strips can be of two varieties: one is comprised of a number of discrete steps ranging from black to white [Fig. 4(a)]; the other is formed by a smooth gradient [Fig. 4(b)].
2. (A). If discrete steps are provided, count the number of steps for which a change in brightness can be distinguished. Record this number. (B). If a gradient is provided, use the digital calipers to measure the length of the strip for which the gradient is visible. Record this distance.

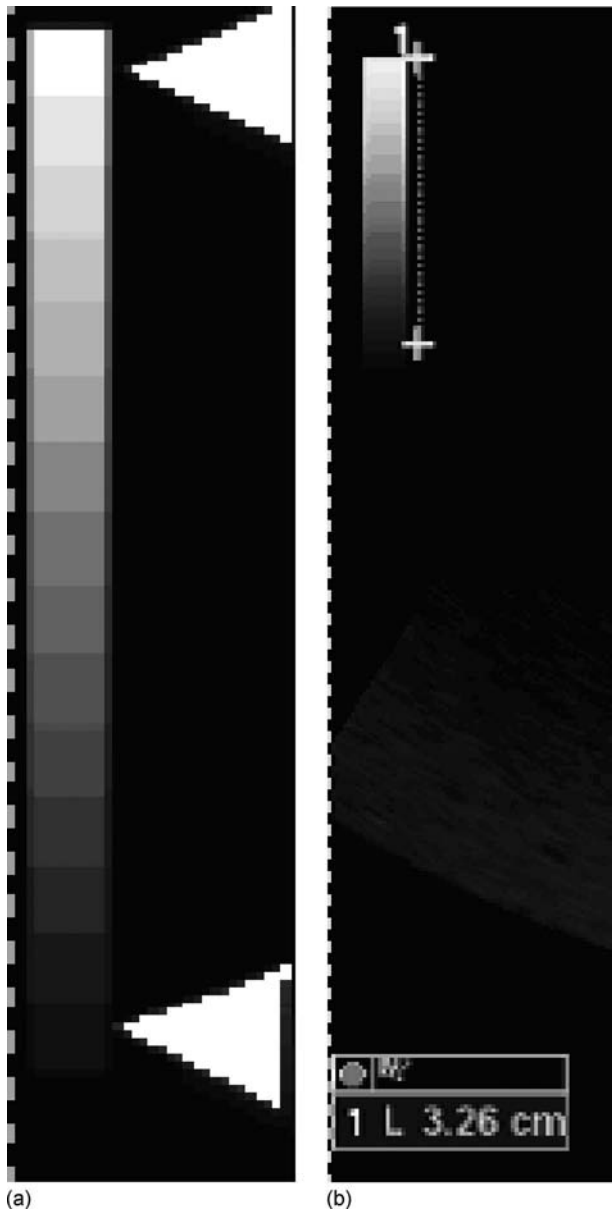


FIG. 4. Grayscale determination. (a) Measurement using discrete steps. The arrowheads indicate the maximum range of discrete steps visible. (b) Measurement using a grayscale gradient. The limits of the visible range are indicated by the plus signs and the length between them indicated at the bottom of the image.

Action limits: The number of discrete steps should not change by more than two, or the gradient length should not change by more than 10% from the baseline image acquired during acceptance testing or at the establishment of the QC program. If a larger change is observed, the monitor should be calibrated according to the operator's manual or reference 2.

II.B. Test 2. Depth of penetration

II.B.1. Recommended frequency: Annual or following transport to another facility

This test measures the sensitivity of the system, which determines how deep into the patient a low contrast object



FIG. 5. Depth of penetration measurement. In this example, the maximum depth, indicated by the x (solid arrow) is approximately 6 cm (dotted arrow). The marker is located at the position where the speckle of the phantom is overcome by the electronic noise of the system.

can be reliably visualized. Any change in the signal to noise ratio (SNR) will impact this measurement. Changes can be caused by a change in electronic or other noise or in the measured signal. Clinically, a decrease in SNR will decrease the maximum depth of penetration, which will make it difficult to visualize the anterior boundary of the prostate.

1. Place the probe on the scanning surface of the phantom using coupling gel.
2. Find a location in the phantom relatively clear of highly reflective targets.
3. Using the probe frequency most commonly used during implants and the maximum power output, determine the maximum depth that the static ultrasound speckle pattern of the phantom can be clearly distinguished from the dynamic electronic noise. If a phantom with low contrast targets at depth is used, these targets can help to distinguish the maximum depth of penetration, for they will disappear when the limit has been reached. Freeze the image and record the scan settings.
4. Using the electronic calipers, measure this depth (Fig. 5).
5. Switch the probe to the orthogonal plane and repeat steps 1–4.
6. Optionally, repeat steps 1–6 at other available frequencies.

Action limit: The maximum depth of penetration should not change by more than 1 cm from the baseline value. While the cause of a substantial increase in penetration should be investigated, of greater concern is a loss of depth of penetration.

Recall that the maximum depth of penetration is impacted by the frequency of the ultrasound being used. Penetration is inversely proportional to the frequency, as ultrasound is attenuated in normal tissue at approximately 0.5 dB/cm/MHz. If anterior structures are not visualized adequately during a case, improvement may be achieved by decreasing the ultrasound frequency, if such selection is available with the ultrasound system. Note that such a change will come at the expense of axial resolution.

It is possible that the maximum depth of penetration might exceed the depth of the phantom, meaning that the full depth of the phantom is well visualized. In this case, one may either use a larger phantom to quantify the performance, or record the maximum depth result as the dimension of the phantom. In the latter case, future testing should verify that the full depth of the phantom remains visible. As commercial phantoms will likely have sufficient depth to represent clinical geometries, this is not likely to be a clinical liability.

II.C. Test 3. Axial and lateral resolution

II.C.1. Recommended frequency: Annual or following transport to another facility

While ultrasound guidance of prostate implants does not depend as critically on spatial resolution as do some diagnostic studies, certain aspects of the procedure can place a demand on the resolution of the system. Poor resolution will make it difficult to properly identify and locate implanted seeds, or the image of a needle may be too spread out to accurately register its location. Spatial resolution can be negatively impacted by poor probe condition and faulty pulse/receive electronics.

It is desirable to perform this test both near the transducer, 1–2 cm into the phantom, and at depth, 5–6 cm into the phantom if targets are available.

1. Find a region of the phantom having single filament targets at various depths (Fig. 6). Alternatively, find a region of the phantom having a region of filament targets positioned successively more closely to each other in the axial and lateral directions (Fig. 7).
2. If the ultrasound unit has variable focus depth, place the focus of the beam at the depth of the targets to be measured (refer to the operator's manual for instructions). Set the gain controls to optimize the visibility of the targets and freeze the image. Record the scan settings.
3. If using single filaments, measure the dimensions of the filament image in both the axial and lateral directions [Figs. 6(a) and 6(b)]. These dimensions are effectively the axial and lateral resolution limits. If using a resolution target group, determine the spacing at which the individual targets are no longer resolved in both the axial and lateral directions (Fig. 7).
4. Switch the probe to the orthogonal direction and repeat steps 1–3 [Figs. 6(c) and 6(d)].

Action limit: The measured axial and lateral resolution should not change by more than 1 mm from the baseline value.

II.D. Test 4. Axial and lateral distance measurement accuracy

II.D.1. Recommended frequency: Annual

To better understand distance accuracy measurements and any associated errors, a brief review of how the ultrasound scanner determines distance is given in Appendix A.

To minimize observer variability, a phantom containing high-contrast fibers is preferred for performing distance accuracy measurements. The phantom should contain at least one column and one row of fiber targets that are separated by a known distance (Fig. 8). If the phantom does not contain such an array of fiber targets, distance accuracies can be adequately measured using objects of known dimensions, such as cylinders or spheres. Note that the size of such objects in the phantom is typically much less than the field of view, restricting the distance range that can be measured and limiting the sensitivity of the measurement. Problematic also with spheres and egg-shaped objects is the partial volume effect. Since there is less target material off of the center of the scan plane, the edges may not be well defined due to the partial volume effect, introducing another potential source of error into the measurement.

When using the electronic calipers for an axial distance measurement, place the calipers centered on or to the left (or right) of the target and centered axially (Fig. 9). On subsequent measurements, be consistent with placing the calipers relative to the targets. For a horizontal distance measurement, the calipers should be placed directly above and centered horizontally over the target image (Fig. 10). It is critical to be consistent in placement of the caliper with respect to the target image.

II.D.2. Axial distance accuracy (Fig. 9)

1. Set the scan parameters such that they are consistent with those used clinically. Record the scan settings.
2. Align a column of fiber targets directly in the center of the image, making sure that the axis of the ultrasound beam is perpendicular to the fibers. Freeze the image. Note: the phantom design may not allow for centering a column of fibers in the field of view. In this case, image a column of fibers and note that a component of any horizontal distance inaccuracy is inherent in the measurement.
3. Using the electronic calipers, measure the distance between the most proximal and the most distal targets.
4. Compute the absolute and percent difference between the known and measured values.

Action limit: Error should be less than or equal to the larger of 2 mm absolute or 2% relative.

II.D.3. Lateral distance accuracy (Fig. 10)

1. Set the scan parameters such that they are consistent with those used clinically. Record the scan settings.

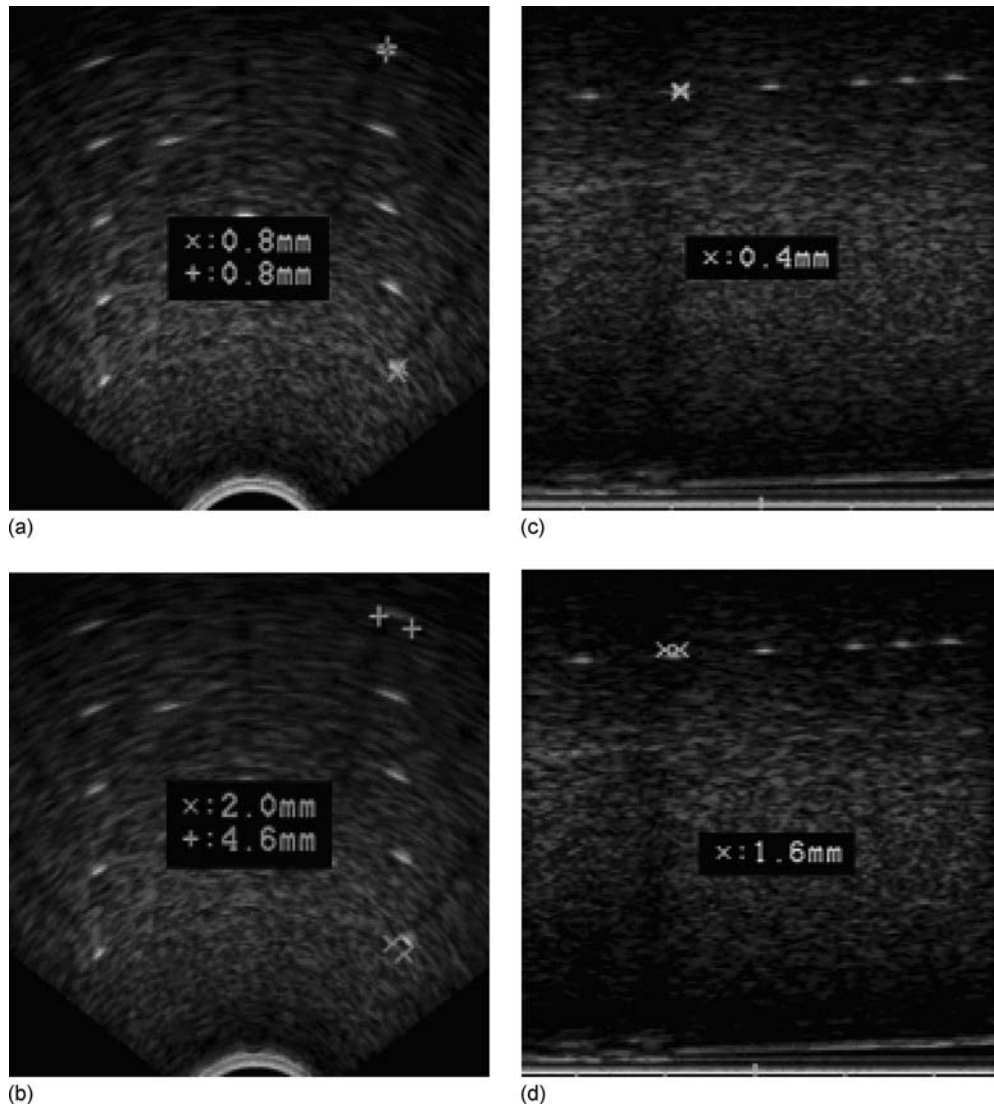


FIG. 6. Resolution using single filament targets. In (a), axial resolution is demonstrated with the axial array, while (b) demonstrates lateral resolution with the axial array. In (c) axial resolution using the longitudinal array is demonstrated, and (d) demonstrates lateral resolution using the longitudinal array. Note the loss of lateral resolution with depth in (b) due to the targets being out of the focal zone of the transducer. Axial resolution is seen to be constant with depth in (a) as axial resolution is primarily dependent upon the frequency of the transducer.

2. Image a row of targets and freeze the image. Make sure that the axis of the ultrasound beam is perpendicular to the fibers.
3. Using the electronic calipers, measure the distance between the left-most and right-most targets.
4. If several rows of fiber targets are available, perform the measurement for the most proximal and most distal rows as in Fig. 10.
5. Compute the absolute and percent difference between the known and measured values.

Action limit: Error should be less than or equal to the larger of 3 mm absolute or 3% relative. Action limits for lateral distance accuracy are greater than for axial accuracy due to the increased number of factors impacting the measurement. Specifically, the reduced spatial resolution in the lateral direction leads to increased uncertainty in the position of the filament.

If high contrast fibers are not available, use the following procedure for circular or other targets with known dimensions.

1. Adjust the system to clinically relevant settings. Scan the object such that the ultrasound beam intercepts the object through a known dimension. For cylindrical objects, make sure that the beam is perpendicular to the axis of the cylinder. Freeze the image and record the settings used.
2. Place the calipers at the top and bottom of the target image and record the measurement [Fig. 11(a)].
3. Place the calipers at the left edge and right edge of the target image and record the measurement [Fig. 11(b)].
4. Compute the percent difference between the known and measured values in each direction.

Action limits: Error should be less than or equal to the

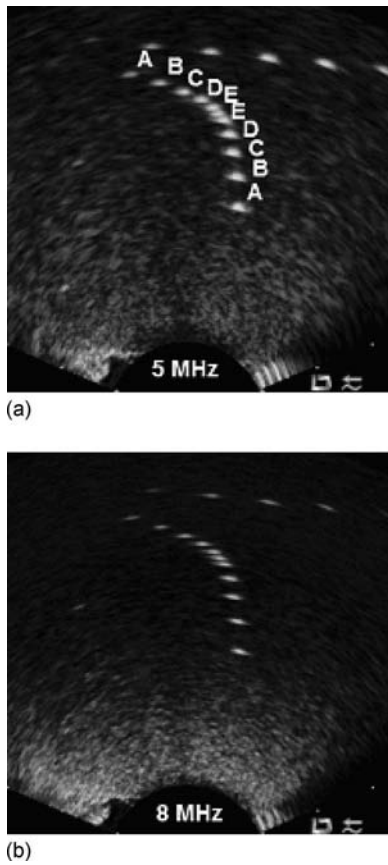


FIG. 7. Resolution using paired filament targets. The axial and lateral separation of the 0.1 mm nylon fibers are A=5 mm, B=4 mm, C=3 mm, D=2 mm, E=1 mm. A transducer frequency of 5 MHz is used in (a) and 8 MHz in (b). Note the improved axial resolution with the higher frequency in (b).

larger of 2mm absolute or 2% relative in the axial direction and less than or equal to the larger of 3 mm absolute or 3% relative in the lateral direction. As above, the lateral boundaries of the target may be more blurred than the axial bound-

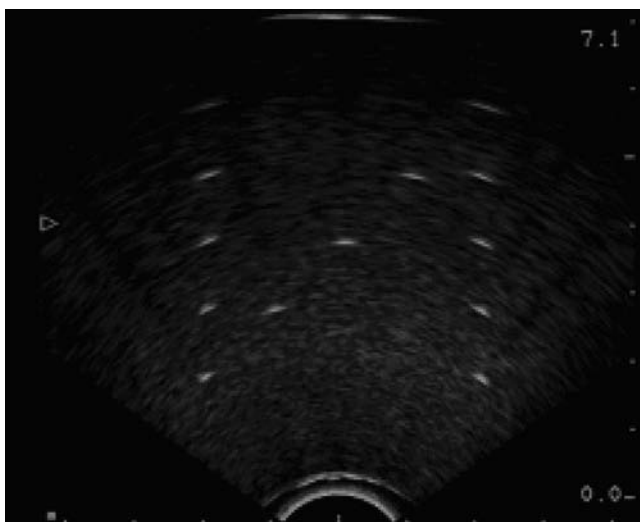


FIG. 8. Phantom containing high contrast fibers for distance verification.

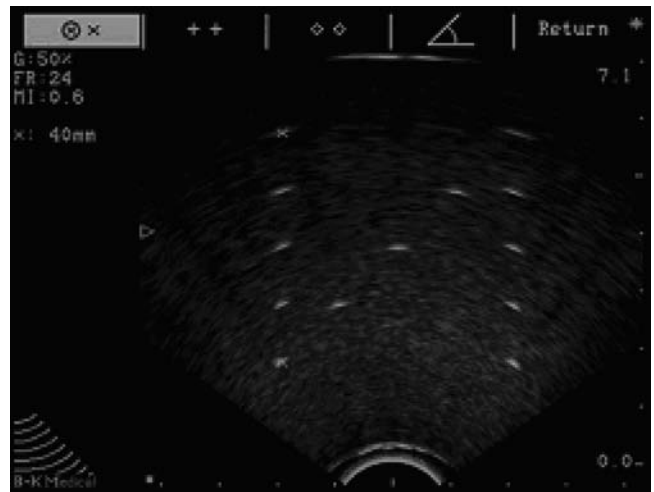


FIG. 9. Axial distance measurement accuracy. Ideally, the fibers should be centered in the field of view. If this is not possible, image a column of fibers and note that the horizontal spatial calibration also contributes to the measured vertical distance. When using the electronic calipers for a vertical distance measurement, place the caliper centered on or along the right or left side (be consistent) and centered vertically with respect to the target image.

aries, so a larger tolerance is allowed for the lateral direction.

Some prostate ultrasound scanners offer the ability to superimpose a square grid of coordinates on the real-time image. The grid coordinates are referenced when designing the treatment plan. Since the grid is created by the scanner regardless of the material that is being imaged, the distance measurements between grid points should be exact. Therefore, the grid overlay is also a useful means to visualize distance inaccuracies throughout the field of view, providing that a phantom with several fiber targets is used. Figure 12 shows a phantom with pins that are spaced apart by 1 cm. The grid points on the overlay are also 1 cm apart. In this

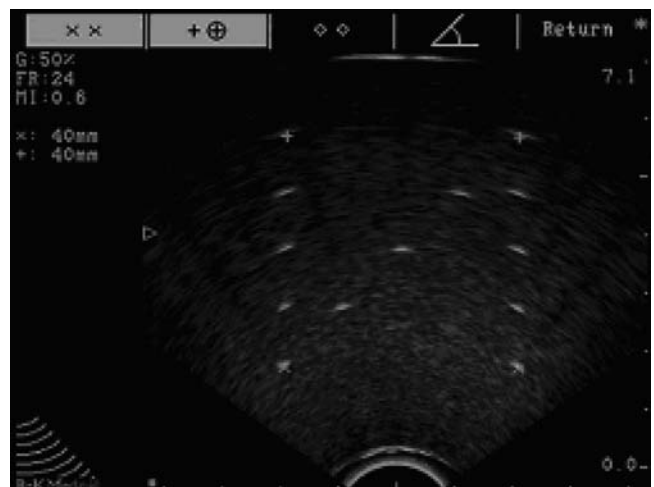
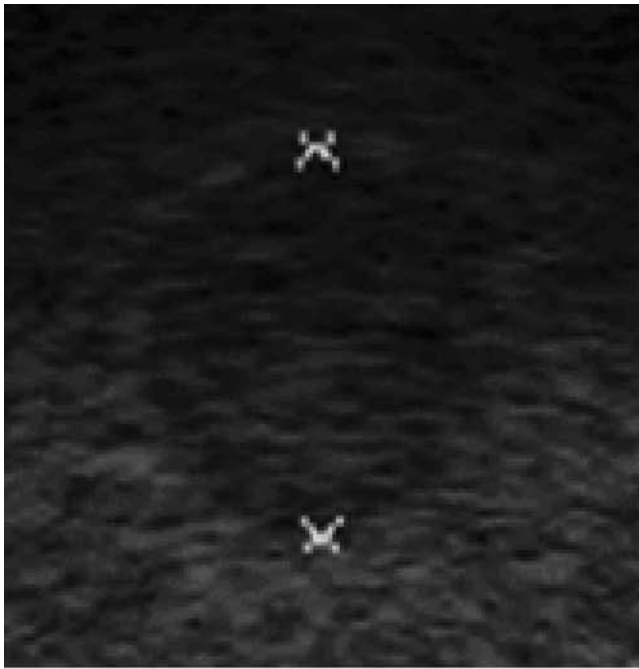
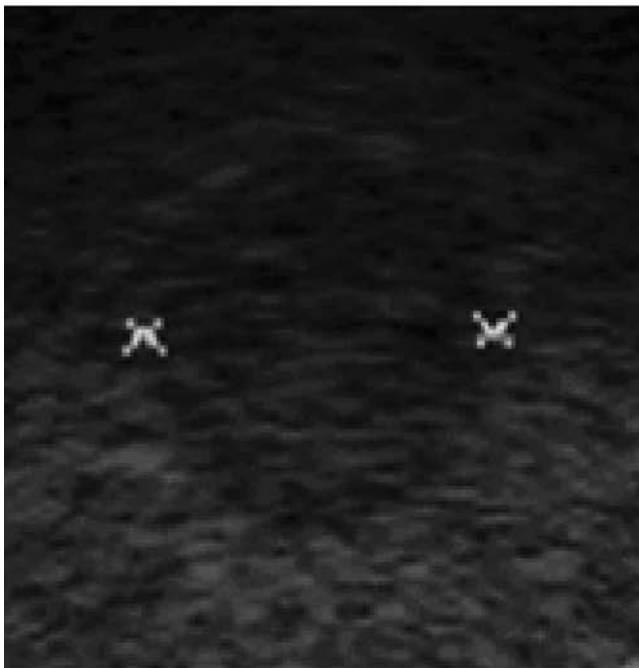


FIG. 10. Measurements of horizontal distance accuracy when several rows of targets are available. For a horizontal distance measurement, the calipers should be placed just above or below the target and centered horizontally with respect to the target. It is critical to be consistent in placement of the caliper with respect to the target image.



(a)



(b)

FIG. 11. Distance accuracy measurements using a cylindrical, sphere, or egg-shaped object. (a) Axial distance measurement; (b) lateral distance measurement.

case, the lateral distance accuracy is worse near the transducer, which is most likely caused by the probe not being orthogonal to the fibers. If the probe is properly orthogonal to the fibers and this appearance remains, some ultrasound systems provide the capability to adjust the grid to bring them into correspondence.

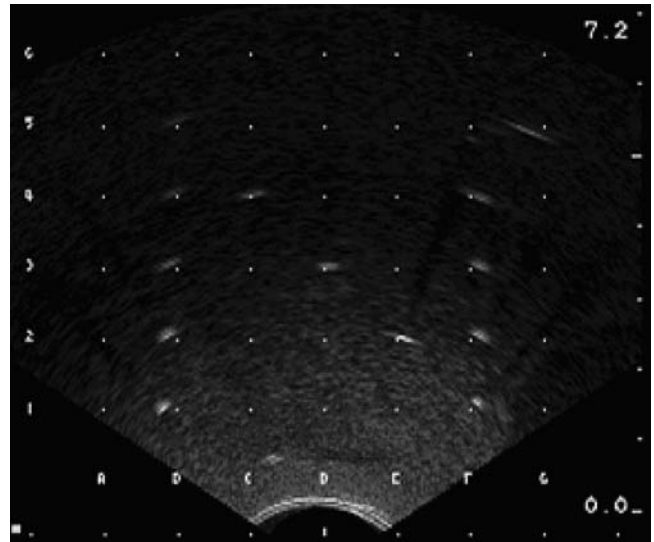


FIG. 12. Using an electronically generated grid to verify distance accuracy throughout the field, of view. Note that fibers near the transducer are rendered farther apart than corresponding grid points. The lateral distance registration at deeper depths is more accurate.

II.E. Test 5. Area measurement accuracy

II.E.1. Recommended frequency: Annual

As the correct calculation of the volume of an object depends upon the accurate determination of the area of an object in the scan plane, area measurement accuracy must be verified. This test requires a phantom with an object with a circular cross section of known size.

1. Adjust the system to clinically relevant settings. Scan the object such that the ultrasound beam intercepts the object through a known dimension. For cylindrical objects, make sure that the beam is perpendicular to the axis of the cylinder. Freeze the image and record the settings used.
2. Using the appropriate tool on the ultrasound system, carefully trace the boundary of the object (Fig. 13).
3. Record the area of the object as calculated.
4. Compute the percent difference between the known and measured areas.

Action limit: The calculated value should be within 5% of the nominal target area.

II.F. Test 6. Volume measurement accuracy

II.F.1. Recommended frequency: Annual

Particularly important for real time dosimetry is the ability of the system to accurately determine the volume of a target. This test will require both a phantom with a three-dimensional target of known size and the stepper used during clinical procedures.

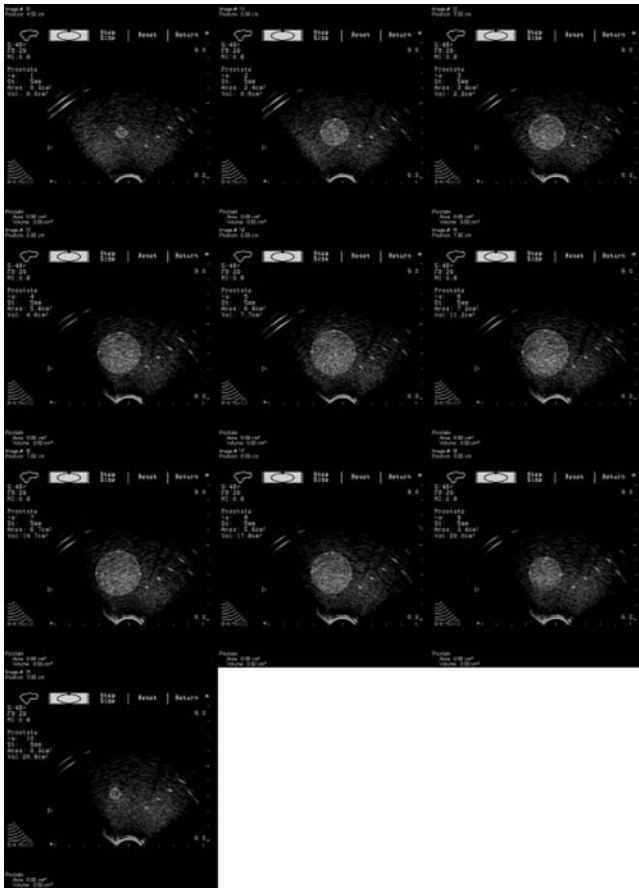


FIG. 13. Volume measurement using a target of known volume.

1. Set up the phantom in a location so that the stepper can maintain good contact between the probe and the scan surface. Apply coupling gel to the scan surface.
2. Locate the equivalent of the base and apex of the phantom target and zero the stepper at the base.
3. Using the typical clinical procedure, translate the probe, contouring the target at each step location, through the target (Fig. 13).
4. After contouring the entire target, record the calculated volume.

Action limit: The calculated value should be within 5% of the nominal target volume.

II.G. Test 7: Needle template/electronic grid alignment

II.G.1. Recommended frequency: The first time a template is used and annually thereafter for preplanned implants, a vendor's disposable templates should be checked periodically for consistency, optional for intraoperative planning

The electronic grid generated by the ultrasound system provides a reference for needle locations in the treatment plan. For preplanned procedures, it is important to verify that the electronic grid overlay matches the location of the actual

needle template. If this alignment is not correct, needles cannot be physically inserted according to the preplan, requiring intraoperative corrections to the preplan.

It should be noted that, even if the template and grid are physically well aligned, some discrepancy may be observed. In clinical use, a beveled needle tip may deflect from the path initiated by the physical template.¹⁴ This may account for discrepancies seen between on-screen template correspondence in water and in tissue.

Currently, no generally available commercial phantom is available for this test; therefore, it is necessary to have the ability to place the stepper in a vertical position so that the probe assembly can be immersed in water.¹⁵

1. Obtain a water container with a volume sufficient to immerse the ultrasound probe.
2. Place the probe with the needle template attached in a vertical orientation and immerse the probe.
3. Ensure that the water is room temperature and free of bubbles.
4. Place needles at each corner of the needle template and one at the center.
5. On the ultrasound system, verify that the location of the needle flashes in the image correspond to the locations of the needles on the electronic grid overlay.
6. If inaccuracy is noted, adjustments may be made to the ultrasound probe and grid support in the lateral, AP, and rotational dimensions, as needed.
7. If no adjustments to the grid support are available, the misalignment distances should be noted and corrected for during the implant.

Action limit: Alignment should be correct to within 3 mm.

With reference to Table IV, it should be noted that use of room temperature water, having a sound speed of approximately 1480 m/s, rather than a tissue mimicking material with a sound speed of 1540 m/s, can introduce a distance error of up to 3.7 mm at a nominal depth of 6 cm. This error can be reduced by increasing the water temperature. Using a formula by Bilaniuk and Wong, a water temperature of 48 °C (118 °F) will yield a sound speed of 1540 m/s.¹⁶ However, it should be noted that it is not clear that this elevated temperature will not have a negative impact on the transducer. Another approach is increasing the salinity of the water to approximately 45 parts per thousand, which would yield a sound speed close to 1540 m/s.^{17,18} This amounts to 43 grams (about six tablespoons) of salt per liter. As above, it should be noted that it is not clear that this elevated salinity will not have a negative impact on the transducer.

II.H. Test 8: Treatment planning computer

II.H.1. Recommended frequency: Acceptance testing of ultrasound system and/or treatment planning computer

The final step is to ensure that the geometry assumed by the treatment planning computer matches that of the ultrasound scanner, or the dosimetry plan may not reflect the actual dosimetry of the implanted prostate.

1. Perform a volume study of the three-dimensional target in the ultrasound phantom, contouring each slice and computing the volume.
2. Import the ultrasound images used for the volume study into the treatment planning computer.
3. Retrace the contours from the ultrasound study with the contouring tools in the treatment planning software.
4. Compare the volume rendered by the treatment planning software to the volume calculated by the ultrasound system.

Action limit: The volumes calculated by the ultrasound system and the treatment planning computer should agree to within 5%.

III. ARTIFACTS

Ultrasound imaging produces artifacts that are fundamentally different in appearance and cause than other imaging modalities. The most common of these in prostate brachytherapy imaging, reverberation, is discussed in Appendix D.

Spurious electronic signals may cause a sweeping appearance to the image. Such signals may be the result of the probe connector having become wet and not dried thoroughly. A wet probe connector can be a substantial electrical hazard, so care must be taken to keep it dry, especially during cleaning of the probe.

Poor contact between the probe and the medium can cause dark regions with poor visibility beyond them; see Fig. 14. This can be caused by air bubbles in a water-filled stand-off, insufficient coupling gel, or even stool in the rectum. The solution for most poor contact problems is self-evident, but must be accomplished before continuing the case.

IV. QUALITY CONTROL DOCUMENTATION

A sample QC form has been included as Appendix E.

V. ADDITIONAL TESTS

If the equipment is suspected of suboptimal performance, additional tests may be used to determine possible causes. A complete description of many ultrasound performance tests is available.²

VI. CONCLUSION

The procedures outlined in this document are targeted towards issues that are of primary importance to ultrasound-guided prostate seed implant therapy. Performance measurements of an ultrasound prostate scanner are an essential component of assuring adequate image quality, accurate measurements, and efficient use of the scanner. Additionally, the ultrasound scanner should be thoroughly tested at acceptance of the unit or if other problems are suspected.

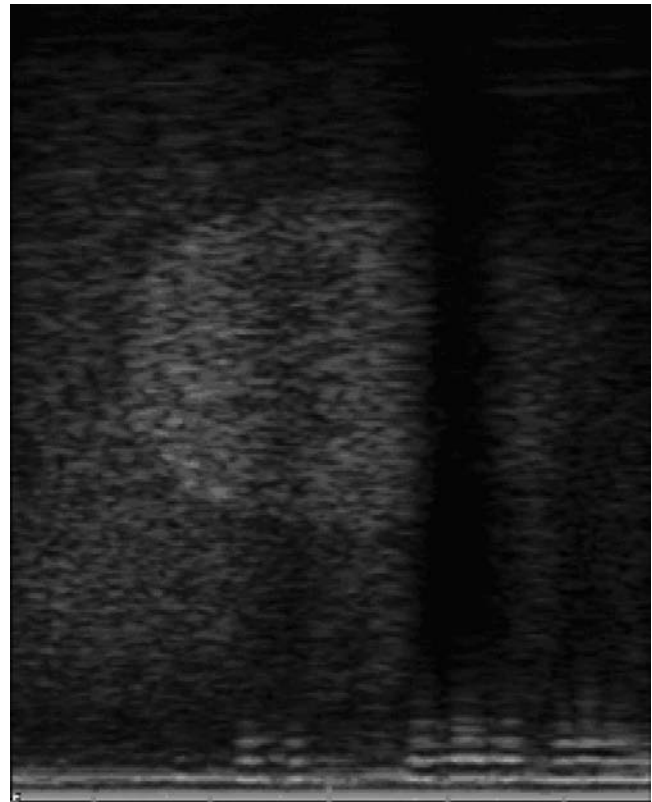


FIG. 14. Artifact caused by poor contact between the ultrasound probe and the scan surface. In this case, the source of poor contact is insufficient coupling gel, leaving an air gap between the probe and scan surface.

APPENDIX A: DISTANCE CALCULATION

1. Axial (vertical) distance measurement

Vertical distance measurements are calculated based on the maximum imaging depth and the height of the image. For example, if the maximum imaging depth is 7 cm and the field of view is displayed using 300 pixels (in the vertical direction), the spatial calibration would be $(300 \text{ pixels}) / (70 \text{ mm}) = 4.28 \text{ pixels/mm}$. Therefore, if the electronic calipers are separated by 100 pixels in the vertical direction, the displayed distance measurement would be $(100 \text{ pixels}) / (4.28 \text{ pixels/mm}) = 23.4 \text{ mm}$. The critical component of the axial spatial calibration is the correspondence of displayed depth to the actual depth within the patient. To determine the depth within the patient, the scanner uses the range equation [Eq. (5) above] where τ is the time between the transmit of the initial pulse and the receipt of the echo and c is the speed of sound in the medium. All clinical ultrasound scanners assume that the medium has a sound speed of 1540 m/s. Therefore, when the operator sets the field of view, the scanner will record echoes for each scan line based on the time required for the echoes to return from the maximum imaging depth. For example, if the maximum imaging depth is 5 cm, echoes originating from 5 cm will reach the transducer

$$\tau = r \times 2/c = 5 \text{ cm} \times 2/154\,000 \text{ cm/s} = 65 \mu\text{s}, \quad (\text{A1})$$

after the pulse has been transmitted. The scanner will transmit a pulse, record echoes for 65 μs , and then transmit a pulse for the next line, assuming that the scanner is maintaining a maximum pulse repetition frequency. If the speed of sound differs from 1540 m/s (Table I), the spatial calibration in the axial direction will not be correct.

2. Lateral (horizontal) distance measurement

The scanner must also determine where the echo data are to be placed on the display in the horizontal direction. Assuming that the spatial calibration of the displayed image is to be identical for the horizontal and vertical directions, the scanner must map the data accordingly. For example, on a linear scanhead, the scan lines are parallel. If the first and last lines are separated laterally by 5 cm, and if the vertical spatial calibration is 3 pixels/mm, the width of the image on the display must be

$$3 \text{ pixels/mm} \times 50 \text{ mm} = 150 \text{ pixels}$$

For sector (“pie-shaped”) scan formats, the scanner must consider the divergence of the scan lines with depth when mapping the data onto the display. For example, consider the following as measured from a clinical scanner. Suppose the first and last scan lines are separated by 45 deg and a physical distance at the face of the transducer of 1.5 cm; the focal point of the sector is 1.3 cm behind the face of the transducer. At a depth of 20 mm, the first and last scan lines are 3 cm apart; at a depth of 60 mm, the first and last scan lines are 6 cm apart. While the corrections for this geometry are inherent to the scanner, this example illustrates that the horizontal distance accuracy can be different at different depths if a system or probe identification error has occurred.

Clinically, distance measurements are important for a number of reasons. First, if distance measurements are in error, then the system is not properly locating objects within the image. Therefore, for example, the locations of needles will not be accurately represented relative to the prostate. Further, it is often important to make accurate measurements during a procedure, such as to determine the distance of a needle from another needle or from the rectal wall. Finally, area and volume measurements, vital to intraoperative planning, are based upon these two primary distance measurements.

APPENDIX B: POSSIBLE SOURCES OF ERROR

An error in a distance or volume measurement can be associated with one or more of the following:

1. Operator related: variability in performing the measurement, including transducer positioning.
2. Phantom related: speed of sound in phantom or phantom defect.
3. Scanner related: scanner malfunction or miscalibration.

TABLE III. Percent error associated with vertical (axial) distance accuracy measurements due to material speed of sound.

	Speed of sound (m/s)	Percent error
Selected tissues		
Soft tissue (average)	1540	0.0
Soft tissue (fatty)	1465	5.12
Soft tissue (nonfatty)	1575	-2.22
Adipose tissue	1450	6.21
Phantom tolerances at 22 °C		
1540 \pm 10 m/s	1530–1550	\pm 0.65
1540 \pm 5 m/s	1535–1545	\pm 0.33
Distilled water		
20 °C	1480	4.05
30 °C	1507	2.19

1. Operator-related errors and uncertainties

The user subjectively determines the caliper placement on a fiber or edge of an object within the phantom. If the object edge is sufficiently defined, caliper positioning can typically be repeatable within one or two pixels. Since the placement of two calipers is required, the deviation may be doubled. This emphasizes the need to measure distances that are as large as possible. Table III provides some examples of the magnitude of error for a distance measurement if the calipers are offset by a given number of pixels.

Another source of operator related error is in the orientation of the transducer. The scan plane must be perpendicular to the target. When imaging a single linear target, its actual depth will be offset by the cosine of the angle the probe makes with the phantom surface (Fig. 15). If spheres or egg-shaped targets are used for area and volume measurements,

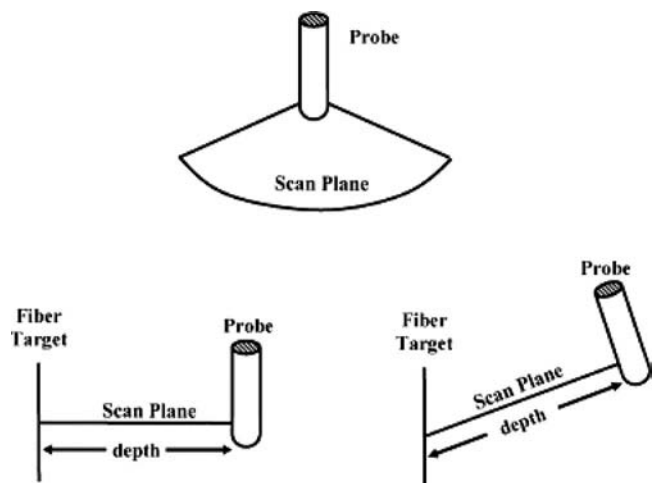


FIG. 15. The displayed depth will not be correct if the scan plane is not perpendicular to the fiber targets. The illustration on the right shows a greater distance from the probe to the target due to the orientation of the probe.

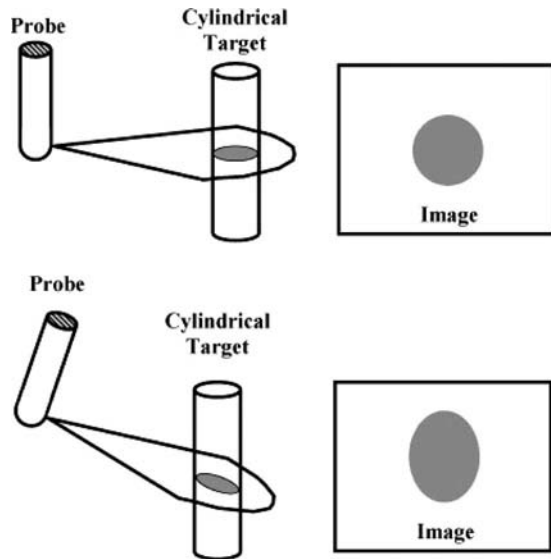


FIG. 16. The top illustration shows the circular cross section of the cylindrical target when the scan plane is perpendicular to the axis of the target. The lower illustration shows an elongated image due to the orientation of the probe. Distance measurements recorded from this image would not correctly reflect the performance of the imager.

the phantom vendor typically provides dimensions for specific cross sections, such as the diameter, major axis, or minor axis. In this case, incorrectly positioning the scan plane can lead to gross distance measurement errors because the imaged cross section does not correspond to the known dimension (Fig. 16).

2. Phantom-related errors

The most common error associated with the phantom is related to the speed of sound in the phantom material. The scanner assumes a speed of sound equal to 1540 m/s. Deviation from a velocity of 1540 m/s will result in an apparent distance inaccuracy. Table IV lists some speeds of sound

TABLE IV. Percent error for distance measurements with various caliper misplacements.

Actual distance (cm)	Off by 1 pixel (% error)	Off by 2 pixels (% error)	Off by 3 pixels (% error)	Off by 4 pixels (% error)
Spatial calibration: 3 pixels/mm				
2	1.7	3.3	5.0	6.7
4	0.8	1.7	2.5	3.3
6	0.6	1.1	1.7	2.2
Spatial calibration: 4 pixels/mm				
2	1.3	2.5	3.8	5.0
4	0.6	1.3	1.9	2.5
6	0.4	0.8	1.3	1.7
Spatial calibration: 5 pixels/mm				
2	1.0	2.0	3.0	4.0
4	0.5	1.0	1.5	2.0
6	0.3	0.7	1.0	1.3

for various materials and the implication on distance accuracy measurements. Note that the speed of sound within all these materials is temperature dependent. For example, one tissue mimicking material experiences a speed of sound decrease of 1.7 m/s per °C drop.² Most phantoms are intended to be used at 22 °C.

3. Scanner-related errors

An error that cannot be associated with the phantom or operator is considered to be the fault of the scanner and corrective action should be taken. Prior to contacting the vendor or a service technician, the user should make additional measurements to assure that the error is repeatable. If the unit is to be serviced, the user may also want to test additional parameters to quantify any other defects in the scanner performance. Testing should also be completed after the unit has been serviced to verify that it is operating properly.

APPENDIX C: BOUNDARY DEFINITION

1. Boundary definition

The lack of a clearly defined prostate boundary on an ultrasound image can affect prostate size and volume measurements along with introducing additional error in matching the preimplant scans to those observed during the seed placement procedure. Boundary definition is determined by four primary factors: axial and lateral resolution, the slice thickness (elevational resolution), and the inherent object contrast of the prostate. Additionally, observer variability in determining the prostate boundary must be considered.

Assuming that there are no partial volume effects, the detail that can be visualized in an ultrasound image is determined largely by the axial and lateral resolutions. However, partial volume effects cannot be neglected when imaging the prostate gland. Therefore, the slice thickness also plays an important role in defining the prostate boundary.

The user has some control over the axial resolution through the choice of transmitted frequency. Higher frequencies yield better axial resolution. The relationship between transmitted frequency and axial resolution is linear (assuming the number of wavelengths in a pulse is held constant). Therefore, a doubling of the transmitted frequency yields a two-fold improvement of the axial resolution. The trade off associated with higher frequencies is attenuation. Attenuation in soft tissue is 0.5–0.7 dB/cm/MHz, which suggests a dramatic increase in attenuation for an increase in transmitted frequency. For example, a frequency of 4 MHz will be attenuated 2 dB per cm of travel, meaning that for every centimeter of travel, the ultrasonic wave loses 37% of its intensity [in units of decibels, the relative intensity of two signals is given by $10 \log_{10}(0.63) = -2.0$ dB]. An 8 MHz beam will be attenuated 4 dB per cm of travel, or 60% of its intensity per cen-

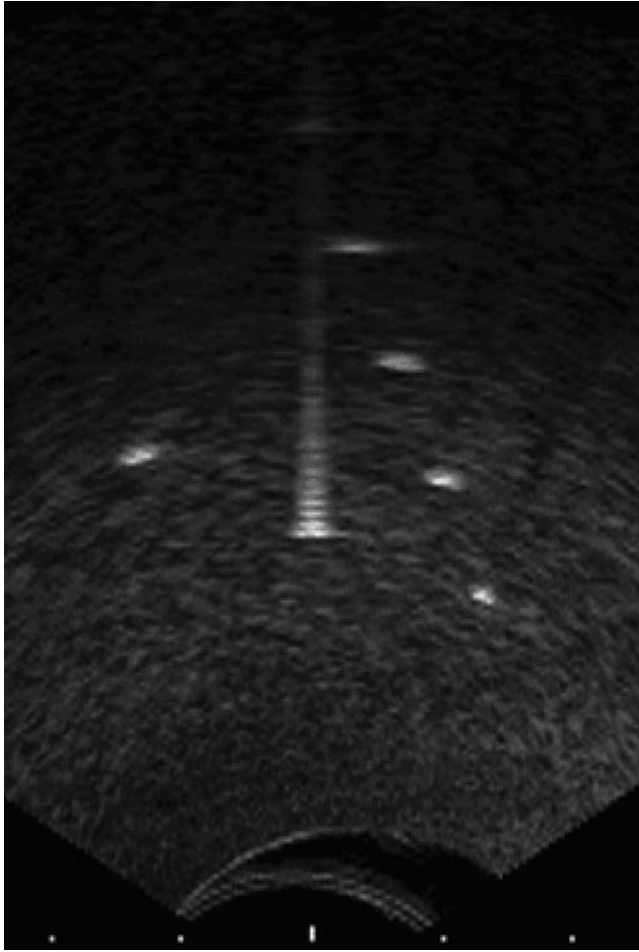


FIG. 17. A ring-down artifact generated by imaging a needle. Note that the “tail” of the artifact always points along a scan line and away from the transducer.

timer of travel. Therefore, the transmitted frequency ultimately determines the depth of penetration of the transmitted pulses. The depth of penetration must be considered when selecting a frequency to optimize axial resolution.

Lateral resolution is influenced by the focal zone placement and by transmitted frequency. To obtain optimal lateral resolution, a focal zone should be placed at the depth of the prostate (or portion of the prostate of interest). Using several focal zones (if possible) can improve the lateral resolution over a larger depth range, but the frame rate will decrease. The decrease in frame rate may, or may not, be objectionable to the oncologist.

Slice thickness is usually not adjustable by the user on systems designed for transrectal prostate imaging.

All of the three resolution dimensions (axial, lateral, and elevational) discussed above can be measured individually; however, the combination of the three determines how the scanner will present the image and how the observer will perceive the image quality. Therefore, measurements of resolution do not provide complete insight to the appearance of the image on the display. Perhaps the best way to approach

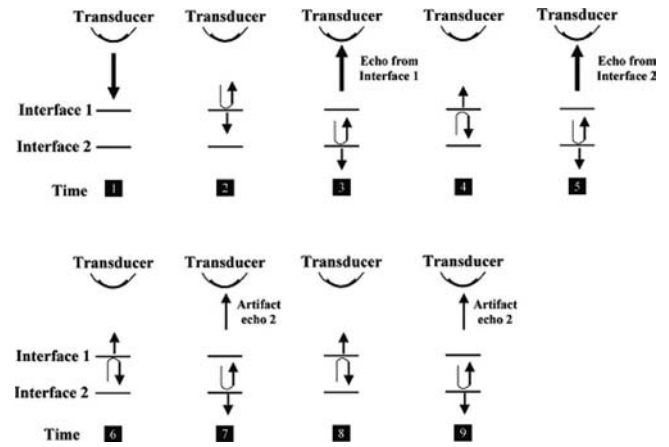


FIG. 18. A time sequence showing the formation of a ring-down artifact. Echoes that correspond to the “true” image of the objects are recorded at the times labeled 3 and 5 in the illustration. However, as the pulse continues to “ping pong” between the two interfaces, additional echoes reach the transducer and appear as equally spaced artifacts on the image. Additionally, the pulse continuously loses intensity as it travels; therefore, the artifact appears to taper off with depth.

the problem is to subjectively evaluate phantom images to become familiar with the uncertainties in defining the prostate boundary. For example, scan a phantom that contains a spherical or egg-shaped object of known dimensions. Using the electronic calipers, measure the diameter (or axis). Remove the probe from the phantom and repeat the exercise. Repeat this sequence until you have an estimate of how precisely you can perform the measurement. Additionally, you could have one or more colleagues perform the measurements. This will also provide insight as to the interobserver variability. Note that the object contrast of the phantom object will affect your results (e.g., a high-contrast object should provide better accuracy and repeatability as compared to a low contrast object). If possible, select a phantom that has been designed specifically for prostate imaging.

APPENDIX D: REVERBERATION ARTIFACTS

1. Reverberation artifacts

The most common artifact in ultrasound-guided prostate seed implant therapy is a ringdown artifact from the needle (Fig. 17). The prominence of the artifact depends primarily on the needle diameter and material. Clinical experience has shown that some types of needles are more susceptible to gross ring-down artifacts than others.

The ring-down artifact is caused by the ultrasonic pulse undergoing multiple reflections between two boundaries (Fig. 18). Little can be done to eliminate this artifact. It is important to be aware of it to minimize its clinical impact.

APPENDIX E: SAMPLE QC FORM*Sample QC form*

Facility _____

System Model: _____ S/N: _____

Probe Model: _____ S/N: _____

Phantom Model: _____ S/N: _____

Name: _____ Date: _____

Grayscale Visibility

Measured number of discrete steps or gradient distance	
Baseline value	

(Action limit: change >2 steps or 10% of baseline value.)

Depth of Penetration

	Axial Plane	Longitudinal Plane
Frequency		
Gain/Power setting		
Depth at which speckle pattern can be separated from electronic noise.		
Baseline value		

(Action limit: change >1 cm from baseline value.)

Spatial Resolution

	Axial Plane			Longitudinal Plane		
	Current	Baseline	Difference (abs / %)	Current	Baseline	Difference (abs / %)
Axial Resolution			/			/
Proximal			/			/
Distal			/			/
Lateral Resolution			/			/
Proximal			/			/
Distal			/			/

(Action limit: change >1 mm from baseline value.)

Distance Accuracy

	Axial	Lateral (proximal)	Lateral (distal)	Sketch:
Expected distance				
Measured distance				
Absolute difference				
Percent difference				

(Action limit: Axial – difference > 2 mm or 2% from nominal value; Lateral – difference > 3 mm or 3% from nominal value.)

Phantoms Containing Cylinders, Spheres, or Egg-Shaped Objects**Measurement Accuracy**

	Top-bottom distance	Left-right distance	Area measure	Volume Measure
Expected				
Measured				
Absolute difference				
Percent difference				

(Action limit: difference > 2 mm or 2% of nominal value for distance measurements; difference > 5% of nominal for area and volume measurements.)

Template Alignment / Needle Verification of Grid Overlay

	Template	Grid Overlay
Greatest discrepancy (mm)		
Tolerance		

(Action limit: difference > 3 mm)

Treatment Planning System Accuracy

	Target
Calibrated target volume	
US volume measurement (from “Measurement Accuracy” above)	
TPS volume measurement	
Absolute difference	

Calibrated – TPS	
US – TPS	
Percent difference	
Calibrated – TPS	
US – TPS	

(Action limit: difference > 5% of nominal and of US-calculated.)

^{a)} Author to whom correspondence should be addressed. Electronic mail: dpfeiffer@bch.org

¹Y. Yu, L. L. Anderson, Z. Li, D. E. Mellenberg, R. Nath, M. C. Schell, F. M. Waterman, A. Wu, and J. C. Blasko, "Permanent prostate seed implant brachytherapy: Report of the American Association of Physicists in Medicine Task Group No. 64," *Med. Phys.* **26**(10), 2054–2076 (1999).

²M. Goodsitt, P. Carson, D. Hykes, and J. Kofler, "Real-time B-mode ultrasound quality control test procedures: Report of AAPM Ultrasound Task Group No. 1," *Med. Phys.* **25**(8), 1385–1406 (1998).

³A. Bell, "Radium and cancer," *Science* **18**, 155–156 (1903).

⁴R. Flocks, "Present status of interstitial irradiation in managing prostatic cancer," *JAMA, J. Am. Med. Assoc.* **210**, 328–330 (1969).

⁵H. Holm, N. Juul, J. Pedersen, H. Hansen, and I. Stroyer, "Transperineal 125iodine seed implantation in prostatic cancer guided by transrectal ultrasonography," *J. Urol. (Baltimore)* **130**(2), 283–286 (1983).

⁶H. Ragde, J. C. Blasko, P. D. Grimm, G. M. Kenny, J. Sylvester, D. C. Hoak, W. Cavanagh, and K. Landin, "Brachytherapy for clinically localized prostate cancer: Results at 7- and 8-year follow-up," *Semin Surg. Oncol.* **13**, 438–443 (1997).

⁷H. Ragde, L. Korb, A. Elgamal, G. Grado, and B. Nadir, "Modern prostate brachytherapy: Results in 219 patients with up to twelve years of observed follow-up," *Cancer* **89**, 135–141 (2000).

⁸P. Grimm and J. Sylvester, "Advances in brachytherapy," *Rev. Urol.* **6**(4), S37–S48 (2004).

⁹J. E. Sylvester, P. D. Grimm, J. C. Blasko, J. Millar, P. F. Orio III, S. Skoglund, R. W. Galbreath, and G. Merrick, "15-year biochemical relapse free survival in clinical Stage T1–T3 prostate cancer following combined external beam radiotherapy and brachytherapy; Seattle experience," *Int. J. Radiat. Oncol., Biol., Phys.* **67**(1), 57–64 (2007).

¹⁰B. Angelsen, *Ultrasound Imaging. Waves, Signals and Signal Processing*

(Trondheim, Emantec, Norway, 2000).

¹¹P. Carson, "Physics of ultrasound propagation," *Medical CT and Ultrasound: Current Technology and Applications*, L. Goldman and J. Fowlkes, eds. (Advanced Medical Publishing, Madison, WI, 1995), pp. 1–14.

¹²M. Insana, "Sound attenuation in tissue," *Medical CT and Ultrasound: Current Technology and Applications* L. Goldman and J. Fowlkes, eds. (Advanced Medical Publishing, Madison, WI, 1995), pp. 15–33.

¹³*Medical CT and Ultrasound: Current Technology and Applications*, L. Goldman and J. Fowlkes, eds. (Advanced Medical Publishing, Madison, WI, 1995).

¹⁴G. Wan, Z. Wei, L. Gardi, D. B. Downey, and A. Fenster, "Brachytherapy needle deflection evaluation and correction," *Med. Phys.* **32**, 902–909 (2005).

¹⁵S. Mutic, D. Low, G. Nussbaum, J. Williamson, and D. Haefner, "A simple technique for alignment of perineal needle template to ultrasound image grid for permanent prostate implants," *Med. Phys.* **27**(1), 141–143 (2000).

¹⁶N. Bilaniuk and G. S. K. Wong, "Speed of sound in pure water as a function of temperature," *J. Acoust. Soc. Am.* **93**(3), 1609–1612, as amended by N. Bilaniuk and G. S. K. Wong (1996), N. Bilaniuk and G. S. K. Wong, "Erratum: Speed of sound in pure water as a function of temperature [J. Acoust. Soc. Am. **93**, 1609–1612 (1993)]," *J. Acoust. Soc. Am.* **99**, 3257 (1996).

¹⁷V. Del Grosso, "New equation for the speed of sound in natural waters (with comparisons to other equations)," *J. Acoust. Soc. Am.* **56**, 1084–1091 (1974).

¹⁸B. Dushaw, P. Worcester, B. Cornuelle, and B. Howe, "On equations for the speed of sound in seawater," *J. Acoust. Soc. Am.* **93**, 255–275 (1993).